Journal of Applied Polymer Science

On the inhomogeneous hydration kinetics and stiffness evolution of HNBR-MgO reactive elastomer composites

Meng Qu,[1] Yucun Lou,[1] Dingzhi Han,[2] Ahmed Amr Gewily,[3] Agathe Robisson[1]

[1] Schlumberger-Doll Research, Mechanics and Materials Science, 1 Hampshire St, Cambridge, Massachusetts, 02139

[2]Schlumberger Reda Production System Pte Ltd, Singapore

[3]Schlumberger Rosharon Center, Rosharon, Texas

Correspondence to: M. Qu (E-mail: mqu@slb.com) and A. Robisson (E-mail: arobisson@slb.com)

ABSTRACT: Swellable elastomers are widely used in oilfield industry for sealing and zonal isolation applications. These materials need to sustain a large amount of external load after swelling. A newly developed reactive hydrogenated nitrile butadiene rubber (HNBR) based elastomer composite with magnesium oxide (MgO) as filler can swell and stiffen when exposed to water, which makes it ideal for oil field applications. However, both the filler hydration and the stiffness evolution inside this composite material are observed to be highly inhomogeneous even for samples on the length scale of millimeters. To understand this coupled diffusion-hydration process is critical for applications of these materials with larger length scales. In this work, the hydration kinetics and stiffness evolution of the HNBR-MgO composite are quantitatively studied on microscopic level. The extent of MgO hydration along the thickness of the sample are measured at the different stage of swelling. These results are used to determine the diffusion coefficient of water inside the composite. The diffusivity increases orders of magnitude after the filler hydration. In addition, the modulus change is non-proportional to the degree of filler hydration as demonstrated by instrumented grid indentation on the hydrated composites. © 2016 Wiley Periodicals, Inc. J. Appl. Polym. Sci. **2016**, *133*, 43420.

KEYWORDS: kinetics; oil and gas; reactive elastomer composites; swelling

Received 7 October 2015; accepted 7 January 2016

DOI: 10.1002/app.43420

INTRODUCTION

In the last two decades, the oilfield industry has seen a significant improvement in drilling practices, enabling long horizontal wells. One of the major components used for completing these wells are swellable elastomer composites, or "swell packers". These are elastomer-based parts placed around the oil producing pipe. They swell by absorbing well fluids until contact with the reservoir is achieved, that is, until the annulus is sealed. For examples, in a production application, the compartmentalization achieved by placing several of these packers (up to 40) in the reservoir can improve the oil recovery factor when combined with in-flow control devices. Another example is for stimulation application, in this case the packers allow targeted, efficient placement of fluids and/or proppant for multi-stage fracturing. The swelling of these elastomer composites can be activated in water-based or hydrocarbon-based fluids. However, in some major unconventional reservoirs, hydrocarbon-based fluids show a tendency to damage certain shale formations. To resolve this issue, the need for water-activated swellable elastomer emerged.[1–6]

Swellable elastomers are conventionally composites with swellable polymers as fillers to imbibe fluid and generate volume expansion. Examples include superabsorbent polymer (SAP)/rubber composite that swells in water[1,2] and ethylene propylene diene monomer (M-class) rubber (EPDM)/rubber composite that swells in oil.[4,6] However, these types of swellable composites lose their stiffness significantly through swelling. This limits their applications in operations that require elastomers to sustain large amount of external load.

A better candidate is reactive elastomer composite with cement or metal oxide powders as fillers that can stiffen while swelling.[3,5] When the water molecules diffuse into the composite, they chemically react with the fillers and form hydrates which have a larger volume; consequently, the volume of the composite will increase. More importantly, the stiffness of the composite increases associated with the increased filler volume. For example, Robisson *et al.* added cement particles into the HNBR matrix. After swelling, the calcium and silicon ions react with water to form calcium silicate hydrate (C-S-H) phase. The stiffness of HNBR-cement composites increased up to four times of its initial value and the volume increased 30%.[5] Han *et al.* demonstrated that by adding 40 volume percent magnesium oxide particles into HNBR, up to 100% increase in volume and five times increase in stiffness was achieved.[3]

The key features for the reactive composite, swelling and stiffening, are both correlated with the hydration of fillers, which are controlled by water-diffusion inside the elastomer. As shown in previous work, even with the sample size on the order of millimeters, water diffusion and filler hydration inside the sample is highly inhomogeneous.[3,5] This inhomogeneity is expected to be even more serious for applications with larger length scale. Therefore, quantitative analysis on the evolution of stiffness and filler hydrations on the microscopic level is needed.

In this study, we investigated the hydration kinetics and stiffening mechanism of HNBR-MgO reactive composites using microscopic observations, thermal analysis tools and nanomechanical measurements. To observe the morphology change of the composites during swelling, we obtained scanning electron microscope (SEM) images on the composites over time, and demonstrated the inhomogeneous morphology change of the MgO filler. To further understand the hydration kinetics, we conducted TGA at different layers of the sample, and quantified the extent of MgO particles hydration through the thickness of the composites. By combining this approach with a diffusion-reaction model, we determine the diffusion coefficient of water in the composite as a function of MgO hydration. Finally, we conducted instrumented grid indentation on hydrated composites to directly visualize the non-uniform stiffness evolution through the sample thickness during swelling, caused from the complex diffusion-reaction process. In addition, we proposed a mechanism to explain the stiffness evolution.

To our best knowledge, this is the first study focused on obtaining an understanding of the hydration kinetics and mechanical evolution of this type of reactive composites at the microscale level. These understandings provide reference values for estimating the swelling and mechanical behavior of similar reactive composite systems with different geometries, as well as under more complicated application conditions.

MATERIALS AND METHODS

Materials

The composite studied in this work was compounded using conventional rubber compounding techniques with an internal mixer. The composite is made with 60% (by volume) hydrogenated nitrile butadiene rubber (HNBR, LANXESS), 40 vol % hard-burned MgO (purity around 80%) (Average diameter $D_{50} = 2$ μm) and about 8 vol % other additives such as antioxidant, processing aid, accelerators, vulcanizing agent. The HNBR-MgO mixture was cured and molded into a 2 mm thick sheet. Beam-shaped samples with the dimension of 20 mm × 4 mm × 2 mm were cut from the sheets for testing.

Macroscale Characterization

The HNBR-MgO samples were immersed into a large amount of deionized (DI) water at 82 °C (180 °F), which is a typical downhole well temperature. During water exposure, the MgO particles inside the composite react with water according to following reaction:

$$MgO\,(s) + H_2O\,(l) \rightarrow Mg(OH)_2(s) \quad (1)$$

More water than necessary for the above reaction diffused into the samples related to the high osmotic pressure due to the presence of ions. The unreacted water was removed through drying in ovens at 82 °C for 7 days. In this study, the swelled samples before or after drying are referred to as wet or dried, respectively. The volume change ΔV and the evolution of Young's elastic modulus E of the samples are measured in time intervals from 2 up to 336 h. The volume of sample was obtained with the buoyancy measurement in water. The volume change% ΔV is defined as follows:

$$\Delta V = (V_t - V_o)/V_o \times 100\% \quad (2)$$

where V_o and V_t are the volume of the sample in the initial state and at time t, respectively. At each time interval, three samples were measured to obtain an average ΔV. The variation in ΔV among samples is within 5%. Pure MgO particles were also immersed in DI water at 82 °C for hydration test as a reference, following the same procedure. The particles were then dried in oven at 82 °C for 7 days to remove unreacted water.

The macroscale storage modulus of the samples was measured at different time intervals using dynamic mechanical analysis (DMA, Model Q800, TA instrument). The measurements were conducted under uniaxial tension, with 0.1% strain amplitude at a frequency of 1 Hz. Because the measured loss modulus is relatively small compared to the storage modulus, it is neglected in this study. Hence, the measured storage modulus represents the macroscale Young's elastic modulus of the composites.

Scanning Electron Microscopy

The microstructure of samples at various stages of swelling are investigated using a scanning electron microscopy (JOEL, JSM-6490LV). The samples were cut into thin slices and mounted on carbon tape for better electron conductivity. Images were taken under the backscattering mode at a voltage of 20 kV.

Thermogravimetric Analysis

The hydration kinetics on HNBR-MgO samples were analyzed using a thermogravimetric analyzer (TGA, Q500, TA instruments). During swelling, the hydration of MgO follows eq. (1). The dehydration reaction of $Mg(OH)_2$ takes place at approximately 300 to 400 °C in the ambient pressure according to the following equation:

$$Mg(OH)_2(s) \xrightarrow{300-400\,^{\circ}C} MgO\,(s) + H_2O\,(g) \quad (3)$$

Thus, by measuring the weight loss during dehydration, the amount of MgO that reacted with water in the HNBR-MgO reactive composites can be quantified. In this test, the composites were heated in nitrogen from room temperature to $T = 950$ °C and the weight loss versus T were measured. As the HNBR degradation also occurs at $T = 300$–400 °C, a TGA test on an unhydrated HNBR-MgO composite sample was measured as a baseline reference. The weight loss of HNBR-degradation was subtracted from the total weight loss measured for hydrated samples.

The inhomogeneity of MgO hydration in the composites was studied using the method mentioned above. The hydrated coupon samples (~2 mm in thickness) were sliced into thin layers with a thickness of approximately 0.25 mm. TGA weight loss experiments were conducted on each layer to quantify the extent of MgO hydration through the thickness at different time

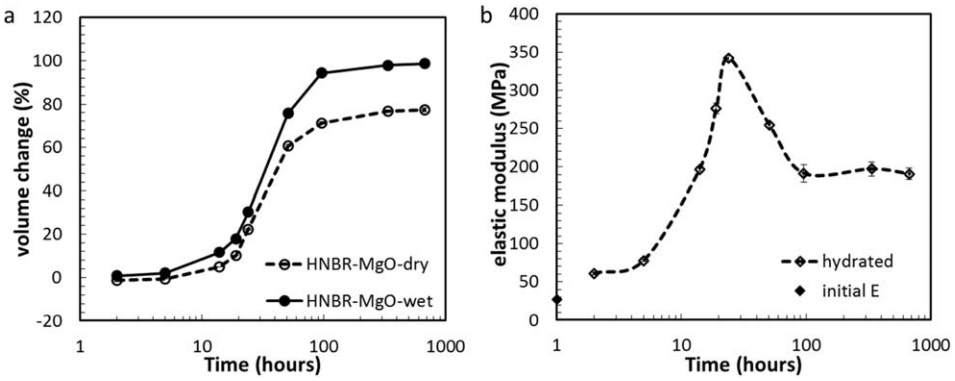

Figure 1. Volume change% ΔV (a) and elastic modulus E (b) of HNBR-MgO composites at different time intervals after being immerged in water. The volume change% ΔV of both wet and dried (i.e., unreacted water removed) samples is shown in (a), E of dried samples is shown in (b). The error bars represent the standard deviation of duplicated samples. The deviations of the tests are small, therefore, the error bars are not visible on some of the plots.

intervals. In this work, we define extent of MgO hydration as the mass percentage of the reacted MgO over the original mass of MgO in the composite. TGA tests were also conducted on pure MgO particles before and after immersing in water for different time intervals (at 82 °C) as a baseline reference. The rate of hydration was calculated using the first derivative over time.

Instrumented Indentation

The inhomogeneity of the elastic modulus during swelling is measured using instrumented indentation (TriboIndenter, Hysitron, Inc) on the samples at different times. A conospherical diamond indenter with probe radius $R=10\,\mu$m was used. The tests were conducted under the load control mode, with a maximum indentation load $P=500\,\mu$N. The maximum indentation depth h ranges from 1 to 3 μm, depending on the stiffness of the samples. Correspondingly, the projected indentation diameter ranges from 9 to 14 μm, which is a relatively large area to capture the modulus of the overall composite at each indent. The loading and unloading time was 10 s with a 10 s dwell time at the maximum load. Grids with 10 × 24 indents were obtained on the cross-section of samples. The grids started from about 70 to 80 μm away from the edge to avoid edge effects.[7,8] The space between each indent was 50 μm. Each indentation map covered about 1.1 mm through thickness, which is at least 50% of the sample thickness. The elastic modulus of the sample before being immersed in water was also measured for reference. Ten indents at different areas were acquired. According to Hertzian's elastic theory, the reduced Young's elastic modulus E_r of each indent was calculated using eq. (4)[9,10]:

$$E_r = \frac{3P}{4h^{3/2}R^{1/2}} \tag{4}$$

The Young's elastic modulus of the composite E was calculated from E_r using eq. (5):

$$\frac{1}{E_r} = \frac{1-\nu^2}{E} + \frac{1-\nu_i^2}{E_i} \tag{5}$$

The Young's elastic modulus E_i and Poisson's ratio ν_i of the diamond indenter are 1070 GPa and 0.07, respectively. The Poisson's ratio of the composite ν is taken to be 0.5, assuming the composite is incompressible.

RESULTS AND DISCUSSION

Macroscale Analysis of Elastic Modulus and Swelling of the Composites

Figure 1(a) shows the macroscale volume change % ΔV of the HNBR-MgO reactive composites, hydrated in DI water at 82 °C up to 336 h, where solid and dash lines represent samples without and with removing the un-reacted water, respectively. The error bars represent standard deviation of duplicated samples. At each time interval, three duplicated samples were tested. The error in the measurements is within 5%, so the error bars are not visible on all of the plots. During the first 5 h, the volume increment is insignificant. An accelerated volume expansion is observed after 5 h up to 51 h. The overall volume of the wet samples increased approximately 75% after 51 h of swelling (before removing the unreacted water). The swelling of the composites slowed after 51 h and reached equilibrium after roughly 96 h, with an equilibrium volume increase of 98 ± 5% (wet samples). The volume increase of the composites was attributed to the hydration of MgO particles as well as the presence of pores from the unreacted water inside the sample. Indeed, if no extra water was diffusing into the sample, the volume increase resulting from MgO hydration only would be 31% (see detailed calculation in 3). This is significantly lower than the observed volume increase (98%). The extra volume increase is related to the additional water that enters the sample. Due to the hydrophobic nature of the rubber, this extra water is expected to diffuse at the interface/inside the magnesium hydroxide islands, making this stiff phase porous.

The hydrated samples were then dried in oven at 82 °C to remove any un-reacted water in the composites. The volume change% ΔV after drying is also plotted in Figure 1(a) (dashed line). It shows that the volume change of the dried samples follow the same trend as the wet samples, with approximately a 20% less volume increase at equilibrium after drying. The relative negligible volume loss after drying the sample further proves that the water was setting mainly in the stiff phase, which did not collapse upon removal of water (i.e., drying within the pores). Note that after drying, the sample mass increase dropped by more than 50%. Further discussions on the porosity within the composites was reported elsewhere.[3] To focus on understanding the hydration behavior of MgO fillers in the HNBR-MgO composites and for simplicity, further experiments and discussions focus on the

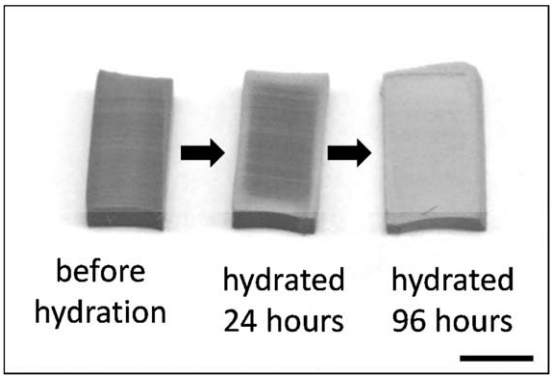

Figure 2. Color change during hydration of the HNBR-MgO reactive composites (cross-section of the samples). Scale bar = 4 mm.

oven-dried samples. that is, after the unreacted water is removed from the composites.

Along with the volume measurements, Young's modulus E of the dried samples was measured using DMA at various time intervals, as shown in Figure 1(b). At the initial stage, the modulus is 27 MPa. The modulus first increases and reaches a peak value of 342 ± 4 MPa at 24 h. The volume change ΔV (after removing of un-reacted water) at this point is about 22 vol % [Figure 1(a)]. With further swelling, the modulus starts to decrease. It becomes 254 ± 3 MPa at 51 h with 61 vol % volume change (ΔV), and reaches 194 ± 8 MPa at equilibrium with $\Delta V = 78\%$ (all modulus measured on dried samples).

Figure 1(a,b) clearly show that the evolutions of the Young's elastic modulus and the volume change of the HNBR-MgO composites do not follow the same trend, which requires a further understanding on the mechanism of stiffness evolution and diffusion-reaction kinetics for these reactive composites. In the following sections, we visualize the microstructure change of the composites before and after swelling using SEM. We then investigate the mechanism of the elastic property evolution and swelling/hydration kinetics of the samples using instrumented nanoindentation and thermal analysis at the microscale. As shown in Figure 1(a,b), the modulus is not monotonically increased with the increasing of the volume. The mechanism of this nonmonotonical stiffness evolution has been further studied through microscopic analysis in Stiffness Evolution section.

Microstructure Evolution during Hydration

Figure 2 shows the cross-section of the HNBR-MgO composite at the initial stage (before swelling), after 24 h and after 96 h of swelling in water. The composite sample at the initial stage had a uniform dark gray color. After the sample was exposed to water for 24 h, the outside layer became lighter in color. After 96 h of swelling in water, the color of the composite changed to light gray throughout its thickness.

The uneven color changes shown in Figure 2 are correlated with the inhomogeneous swelling (and MgO hydration) of the sample. In fact, the morphology images of the HNBR-MgO composites acquired under the SEM, as shown in Figure 3(a–c), confirm a qualitative correlation between macroscopic color and microstructure. Before swelling, crystal-shaped MgO particles are distributed evenly in the HNBR matrix [Figure 3(a)]. After the sample was exposed to water for 24 h, we acquired images [Figure (3b)] of the surface layer and the center of the sample, which correlate to the light color and dark gray color area in Figure 3(b) (inset), respectively. The SEM image on the surface layer of the sample [Figure 3(b), right] showed a higher apparent particle volume percentage comparing to the initial composite. Almost all particles seem to be connected to each other. In the center of the same sample, the particles are still relatively isolated [Figure 3(b), left] and there is no significant morphology difference from the initial state [Figure 3(a)]. After 96 h of swelling, the composite showed a much even morphology, with a high apparent particle loading through thickness [Figure 3(c)]. Thus, from the SEM images, we conclude that the color change at various time intervals is related to the inhomogeneous MgO hydration of the sample. Further analysis to determine the extent of MgO hydration will be discussed in Water Diffusion and MgO Hydration Kinetics in HNBR-MgO Composite and Stiffness Evolution sections.

Water Diffusion and MgO Hydration Kinetics in HNBR-MgO Composite

The volume expansion and stiffness evolution of the HNBR-MgO reactive composite during swelling involves two concurrent processes: 1). water diffusion through the composites. Following Fick's law,[11] the water diffusion time is proportional to the square of the sample length, that is, the larger the sample the longer the time it takes for water to diffuse through it. 2). the hydration of MgO particles in HNBR matrix. The hydration of MgO particles in water is a function of the temperature and the properties of MgO particle, such as the particle surface reactivity and average particle size. As MgO particles are embedded in the HNBR matrix, hydration of MgO can also be limited by the amount of water molecules that are diffused into the composite, for example, hydration rate is expected to be slow in the center of the sample during the early stage due to the lack of

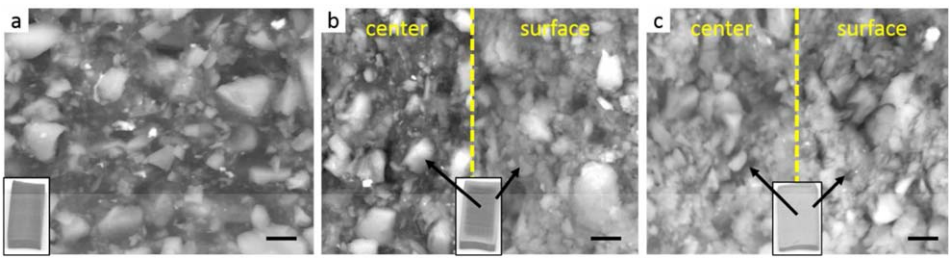

Figure 3. SEM images of HNBR-MgO composites: before immersion in water (a), after 24 h (b) and 96 h (c) of immersion in water. Scare bar = 2 μm. (Insets: optical images of the hydrated composites.). [Color figure can be viewed in the online issue, which is available at wileyonlinelibrary.com.]

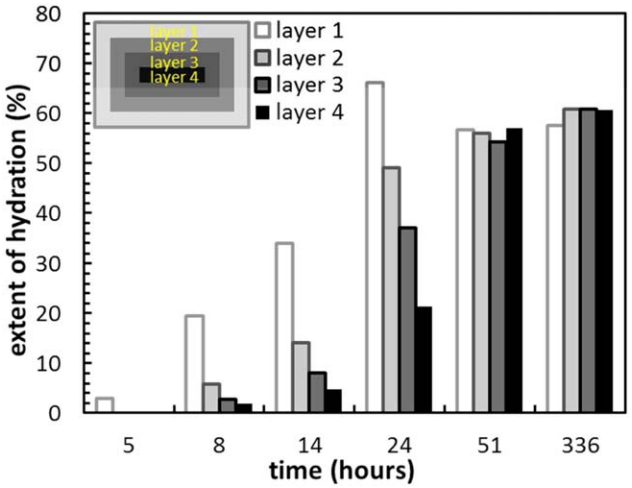

Figure 4. Extent of MgO hydration through the thickness of the HNBR-MgO composites, at time intervals $t = 5$–336 h after immersion in water, measured by TGA. MgO hydration reached equilibrium at $t = 51$ h. [Color figure can be viewed in the online issue, which is available at wileyonlinelibrary.com.]

water. In the following sections, this diffusion-hydration process is analyzed through both experimental measurement and theoretical analysis.

Hydration Kinetics via TGA Test. The extent of MgO hydration in the HNBR-MgO composite; that is, amount of MgO reacted with water normalized by the total amount of MgO in the composites, is measured using the TGA at six time intervals from $t=5h$ up to $t=366h$. The inhomogeneity of MgO hydration through the thickness of the sample was studied quantitatively: at each time interval, the hydrated sample was sliced into four layers along the thickness of the composite from the surface to the center, as illustrated in Figure 4 (inset). The extent of MgO hydration for each layer was estimated using TGA weight loss test (Figure 4). As indicated in the figure, even with the sample thickness as thin as 2 mm, the hydration of MgO fillers is highly heterogeneous within the first 24 h. After 5 h, the hydration is only observed in the surface layer; that is, 3% of MgO was hydrated in layer 1 (surface layer). After 8 h, MgO particles in the center layer starts to hydrate, that is, 2% of MgO hydration in layer 4. The diffusivity of water inside the composite can be estimated using a scaling analysis. Using an estimation of the diffusion length $L=1$mm (half of the sample thickness) and diffusion time of $t=8h$, the diffusion coefficient D of water is as approximated to:

$$D \sim \frac{L^2}{t} \approx 3.5\times10^{-11}\mathrm{m}^2/\mathrm{s} \qquad (6)$$

By comparing the TGA results with the instrumented indentation measurement, we can see that the modulus variation is correlated with the MgO hydration. For example, at $t=24h$, hydration of MgO is highly non-uniform along the thickness, with an average of 66% hydration at the surface layer (layer 1) while only 21% hydration in the center (layer 4). These results are consistent with the modulus evolution through the composite thickness, as will be discussed in Stiffness Evolution section. That is, the elastic modulus at the sample surface is higher than in the center, as most of the MgO particles were hydrated at surface. The reacted MgO [i.e., $Mg(OH)_2$] expands and significantly increases the local stiff filler content, which leads to a higher elastic modulus at the surface. On the other hand, the hydration of MgO is only about 21% in the center, which brings a lower modulus increase in the center of the composite. Note that the extent of hydration never reached 100%. This is mainly due to the lack of purity of the MgO (purity is around 80%). It is also possible that a small amount of MgO filler at the surface of the composites leached out of the sample (see discussions below). Uniform MgO hydration is achieved after 51 h of swelling. Further water exposure confirms that MgO hydration reached equilibrium at around $t=51$ h, as no significant MgO hydration% change was observed between $t=51-366$ h.

It is worth mentioning that about a 10% decrease in the apparent MgO hydration% (56%) was observed at $t=51-366h$ at the surface layer (Figure 4), compared to the 66% of hydrated MgO at $t=24h$. This is related to the certain amount of material loss during hydration (probably ionic leakage and hydroxide leaching from the sample surface layer to the solution). The TGA measurement, not shown here, confirmed that after 51 h of hydration, the total MgO filler content dropped from 40 vol% to about 38 vol % at the surface layer.

Figure 5 compares the extent of MgO hydration with time at surface layer and in the center of the HNBR-MgO composites. This comparison demonstrates that not only is there a delay of MgO hydration in the center of the composites; the hydration rate (slopes in Figure 5) of the filler in the center is also slower than that at the surface. This again confirms that in HNBR-MgO composites, MgO hydration is time-controlled by water diffusion through the thickness. That is, the hydration rate of MgO in the center of the composite decreases due to the limited amount of water reaching the center over time.

Theoretical Analysis. The essential features of HNBR-MgO composite, that is, increasing the volume and stiffness when in contact with water, are both correlated with hydration of MgO fillers. How fast the fillers can react with water depends on the properties of the MgO particles. The reaction time is also limited

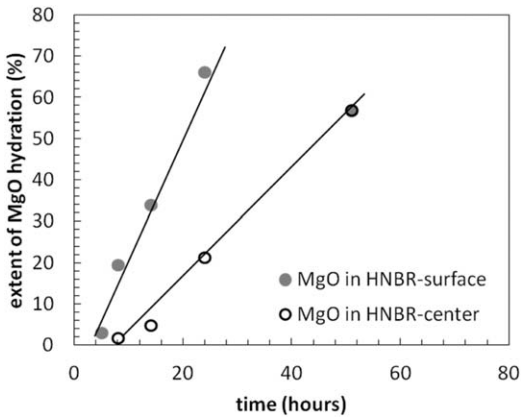

Figure 5. Extent of MgO hydration at surface layer (layer 1) versus center layer (layer 4).

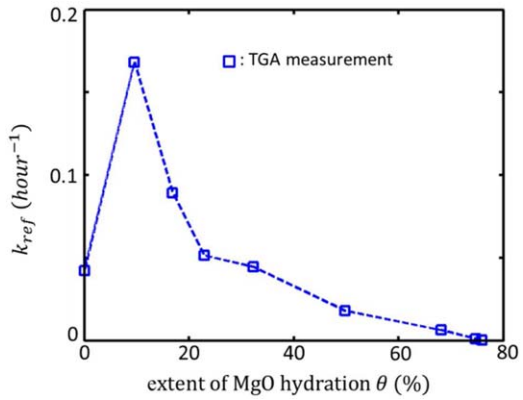

Figure 6. The hydration rate k as a function of the extent of hydration θ of pure MgO particles measured by the TGA weight loss test. [Color figure can be viewed in the online issue, which is available at wileyonlinelibrary.com.]

by the amount of water that surrounds the fillers; for example, the fillers in the center layer hydrate much slower than the fillers in the surface layer as shown in Figure 5. Here, the coupled water diffusion and filler hydration are simulated using a diffusion-reaction model, which is similar to the model developed by Seingol *et al.* on predicting the cement hydration.[12] The diffusivity of water inside the composite is estimated from comparing the modeling results with the experiments.

Consider a representative volume element inside of the composite sample with the location $\boldsymbol{X}$ and at time t, the concentration of liquid water is defined as follows:

$$C(\boldsymbol{X},\, t)=\frac{V_w(\boldsymbol{X},\, t)}{V_e(\boldsymbol{X},\, t)} \tag{7}$$

where V_w and V_e are volumes of water and element, respectively. Therefore, $C=0$ means no water and $C=C_{\text{sat}}$ means that water has reached the saturation value, C_{sat}. Because the matrix phase (HNBR) is highly hydrophobic, water tends to be mainly located inside the porous fillers and at the filler/matrix interface. Therefore, it is anticipated that the value of C_{sat} will increase as more fillers are hydrated. Following Fick's law, the water flux, $\boldsymbol{J}$, is taken to be proportional to concentration gradient according to the following equation:

$$\boldsymbol{J}(\boldsymbol{X},\, t)=D\nabla C(\boldsymbol{X},\, t). \tag{8}$$

where D is defined as the diffusivity of water inside of the composite. Similarly, D is also expected to be affected by filler hydration.

The extent of hydration at each location $\boldsymbol{X}$ and moment t is described with a field variable $\theta(\boldsymbol{X}, t)$, where $\theta=0$ indicates no hydration and $\theta=1$ implies fillers are fully hydrated. The hydration of fillers transforms liquid water into solid $Mg(OH)_2$. Therefore, the hydration process tends to consume water, that is, causing $C(\boldsymbol{X},\, t)$ to decrease. For the degree of hydration to increase from θ to $\theta+\Delta\theta$, the water consumed (volume of water per initial volume of element), defined as C_c, is given by:

$$C_c=\alpha\phi\Delta\theta \tag{9}$$

where α is the molar volume of water (18.1 mol/cm^3) normalized by the molar volume of MgO (11.3 mol/cm^3 for the sample used in this work) and ϕ is the volume MgO filler per volume of element. For simplicity, ϕ is taken to be a constant during hydration. The constants for the material considered in this work are $\alpha=1.6$ and $\phi=0.4$ (initial MgO content).

How fast the fillers react with water, that is, defined as $k=\Delta\theta/\Delta t$, depends on the property of MgO fillers; for example, particle size, but is also limited by the concentration of water. In principle, k increases with increasing temperature and k also varies in the different stages of hydration; therefore, $k=k(\theta,\, T)$. In the swelling experiments discussed in this work, the temperature is constant, so $k=k(\theta)$. When fillers are in contact with enough water, k is assumed to be identical to the hydration rate of pure MgO particles in water, defined as $k_{\text{ref}}(\theta)$. The hydration rate of pure MgO is estimated using the TGA test and plotted in Figure 6. In numerical simulations, the maximum unit volume water consumed due to hydration of MgO from time t to $t+\Delta t$ can be obtained from eq. (10) as follows:

$$C_C=\alpha\phi k_{\text{ref}}(\theta)\Delta t \tag{10}$$

However, if sufficient water is not available, for example, C_C obtained from eq. (10) is larger than $C(\boldsymbol{X},\, t)$, k has to be smaller than k_{ref} to avoid the concentration field from becoming negative. In that case, we assume $C_c=C(t)$. Consequently, $k(\theta)=\frac{C(t)}{\alpha\phi\Delta t}$; therefore, the hydration rate can be determined from the following equation:

$$k(\theta,\, t)=\min\left\{k_{\text{ref}}(\theta),\, \frac{C(t)}{\alpha\phi\Delta t}\right\} \tag{11}$$

The water-diffusion and MgO-hydration are coupled with the conservation of mass:

$$\frac{\partial C}{\partial t}(\boldsymbol{X},t)=\nabla\cdot\boldsymbol{J}(\boldsymbol{X},\boldsymbol{t})-\alpha\phi k(\theta,\, t) \tag{12}$$

The degree of hydration in each volume element is given by:

$$\theta(X,\, t)=\int_0^t k(\theta,\tau)d\tau \tag{13}$$

Initially, the sample is assumed to be dry and unhydrated. Therefore, the initial condition is given by:

$$C(\boldsymbol{X},\, 0)=0 \text{ and } \theta(\boldsymbol{X},\, 0)=0 \tag{14}$$

When the sample is immersed into water, the water concentration near the sample surface tends to reach saturation instantaneously. Therefore, the boundary condition can be given by the following equation:

$$C\,(\boldsymbol{X},\, t)=C_{\text{sat}} \text{ for } \boldsymbol{X} \text{ on the surface}. \tag{15}$$

The water distribution, $C(\boldsymbol{X},\, t)$, and filler hydration, $\theta(\boldsymbol{X}, t)$, for the composite is governed by eqs. (12) and (13). These governing equations are solved numerically using the finite difference method associated with the initial condition, eq. (14) and the boundary condition, eq. (15). For a given time step Δt, the hydration rate $k(\theta,\, t)$ is determined by eq. (11) to take into account the limited water availability inside the composite.

The coefficients that need to be specified for this model include the saturated concentration, C_{sat}, and the water diffusivity, D. As discussed in previous section, the composite tends to be more porous when more fillers are hydrated. Therefore, C_{sat} and D are expected to be a function of the extent of hydration

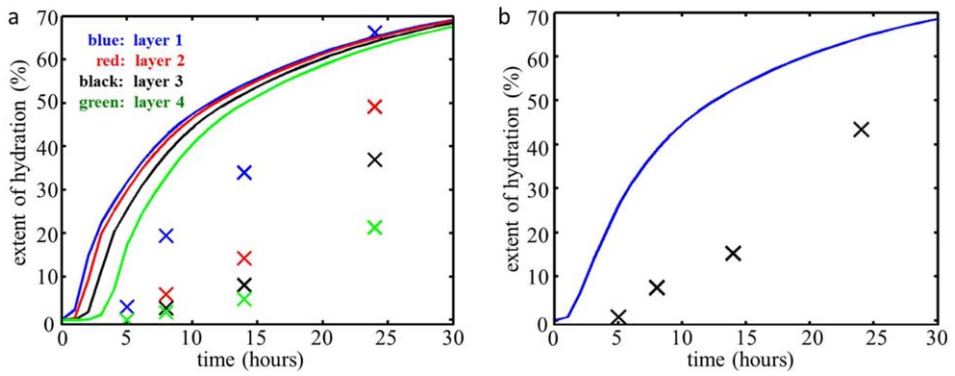

Figure 7. Comparison between numerical results (solid curves) and TGA experimental results (crosses) in case 1, where (a) is the MgO hydration in each layer and (b) is the total hydration of the samples (i.e., the average of all layers). [Color figure can be viewed in the online issue, which is available at wileyonlinelibrary.com.]

of the MgO fillers. For simplicity, C_{sat} and D are taken to be proportional to the extent of hydration, that is,

$$C_{sat}(\theta) = C^I_{sat} + \left(C^E_{sat} - C^I_{sat}\right)\theta(X,\ t) \tag{16}$$

$$D(\theta) = D^I + \left(D^E - D^I\right)\theta(X,\ t) \tag{17}$$

where the superscript I and E refer to the initial and equilibrium values, respectively. The values of C^I_{sat} and C^E_{sat} are estimated from drying tests of the swelled samples. For a swelled sample with the volume V_s and mass change Δm after drying, the volume concentration of saturated water can be estimated as follows:

$$C_{sat} = \frac{\Delta m}{\rho_W V_s} \tag{18}$$

where ρ_W is the density of water. Using eq. (18) and mass and volume changes of x at 0+ h and y at 54 h, C^I_{sat} and C^E_{sat} is estimated to be 0.001 and 0.30, respectively. It is worth emphasizing that C_{sat} cannot be measured directly through the volume change by drying the free-water since porous structure will not fully collapse after water is fully evaporated. The diffusion coefficient D^I and D^E, are determined through fitting with experiments. Indeed, we can show that the simple estimate of a unique value of diffusivity through scaling analysis that is given by eq. (6) cannot predict the inhomogeneity of sample hydration. In fact, we will show that diffusivity changes orders of magnitude after hydration of fillers.

First, we can check the hypothesis of a unique diffusivity. Here, we use the diffusivity estimated from scaling analysis given by eq. (6), as a reference. In this case, we assume:

$$D^E = D^I = 3.5\times10^{-11}\,\mathrm{m^2/s} \tag{19}$$

The modeling results based on this assumption are plotted as solid curves in Figure 7(a) for hydration of MgO in each layer and Figure 7(b) for the hydration of the sample (i.e., the average of all layers). Comparing to the experimental results [crosses in Figure 7(a,b)], the model overestimates the kinetics of MgO particle hydration in HNBR rubber. As shown in Figure 7(a), the modeling results predict that the hydration is nearly homogenous at $t = 24$ h, that is, the solid curves nearly overlap, while experimental results show that the hydration is still highly nonuniform. In addition, the overall hydration rate for the sample measured experimentally is much slower than that predicted by the modeling, especially in the early stage ($t < 5$ h), as shown in Figure 7(b). All of the results indicate that a constant diffusivity assumption cannot fit experimental observations.

Now, let's assume that diffusivity evolves with the extent of hydration. In this case, D^I and D^E are varied to best fit the total hydration rate measured from experiments using the least-square root method. The values of D^I and D^E are determined as follows:

$$D^I \approx 7\times10^{-14}\,\mathrm{m^2/s}\ \text{and}\ D^E \approx 3\times10^{-10}\,\mathrm{m^2/s}. \tag{20}$$

The comparison between experiments and modeling are shown in Figure 8(a, b), which shows that the modeling results are more consistent with experiments than in the first case. By assuming that the diffusion coefficient is low ($10^{-14}\mathrm{m^2/s}$) at the beginning and high ($10^{-10}\,\mathrm{m^2/s}$) after hydration, we can predict the initial slow hydration ($t < 5$ h) and the nonuniform hydration between layers observed from experiments, as shown in Figure 8(a). Furthermore, we can match the total hydration of the sample as a function of time, as shown in Figure 8(b). The diffusivity D^I is low initially ($10^{-14}\,\mathrm{m^2/s}$), which indicate the composite is highly hydrophobic and dense. The diffusivity is high in equilibrium ($D^E = 10^{-10}\,\mathrm{m^2/s}$), which is consistent with the experimental observations that the fillers and filler/matrix interfaces become porous after hydration.

From the cases studied, we have demonstrated that the hydration of MgO fillers inside of the HNBR composite can be captured by a diffusion-reaction model. By assuming that the saturated water concentration and diffusivity are linearly dependent on the extent of hydration, we have shown that the modeling results are in good agreement with experiments. These hypotheses still need to be validated in separate experiments, which is beyond the scope of this work.

Stiffness Evolution

The inhomogeneities in MgO hydration observed through the thickness of the sample results in inhomogeneities in composite stiffness. Modulus maps through sample thickness were measured using instrumented indentation on samples swelled for 24, 51, and 96 h [Figure 9(a–c)]. On these maps, E was measured locally starting from near the edge ($x \approx 0$) and to the center

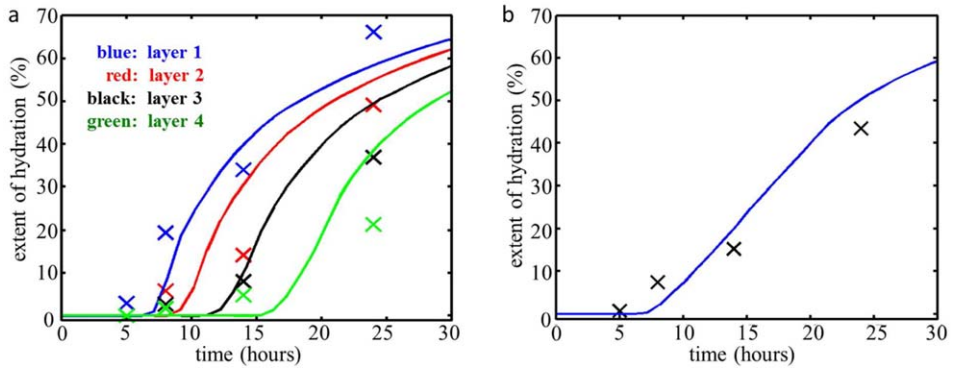

Figure 8. Comparison between numerical results (solid curves) and TGA experimental results (crosses) in case 2, where (a) is the MgO hydration in each layer and (b) is the total hydration of the sample (i.e., the average of all layers). [Color figure can be viewed in the online issue, which is available at wileyonlinelibrary.com.]

($x = 1150$ μm) of the samples. It is worth mentioning that to avoid any edge effect,[7,8] the first row ($x \approx 0$) of the indents is approximately 70–80 μm away from the sample edge. Figure 9(d–f) illustrates the average E of each row. The local E (22 ± 1 MPa, average of 10 measurements) of the composite before swelling is also plotted. Note that the elastic modulus obtained via instrumented indentation is comparable to the E measured using DMA (27 ± 1 MPa). Detailed experimental methods are in Instrumented Indentation section.

The local elastic modulus map of the composite at 24 h of water exposure is shown in Figure 9(a). The average E of each row is shown in Figure 9(d). At this swelling time, the composite reached its peak macroscale modulus value [342 ± 4 MPa, Figure 2(b)]. It is clear that there is a modulus gradient after the samples was exposed to water for 24 h. The Young's modulus at $x = 0 - 50$ μm is 320 ± 27 MPa, at $x = 350 - 1150$ μm is on the average of 85 ± 3 MPa, and at $x = 1150$ μm is 69 ± 5 MPa. Note that even the lowest local modulus in the center is

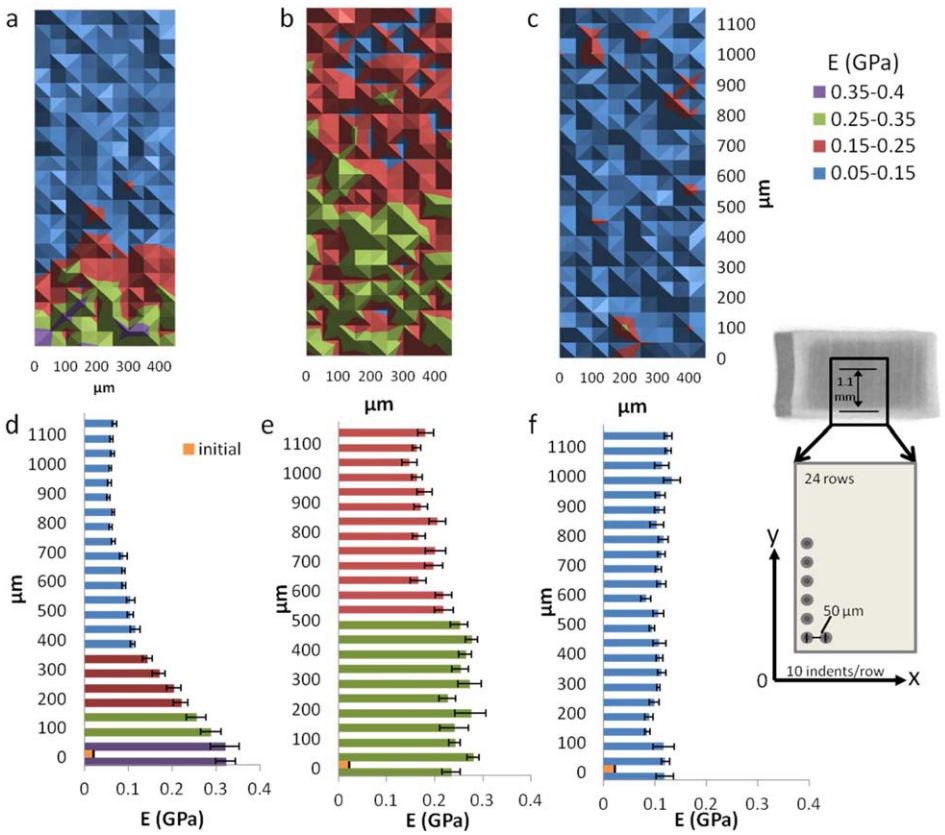

Figure 9. Grid instrumented indentation modulus maps (10 × 24 indents) of the HNBR-MgO composites exposed to water for (a) 24, (b) 51, and (c) 96 h. The Y-axis represents the distance from near the edge ($y \approx 0$, in practical it is about 70–80 μm away from the edge) to the center ($y = 1150$ μm) of the composites. The X-axis represents the ten indents in each row, with 50 μm spacing between each indent. The average E of each row are shown in (d, e, f). [Color figure can be viewed in the online issue, which is available at wileyonlinelibrary.com.]

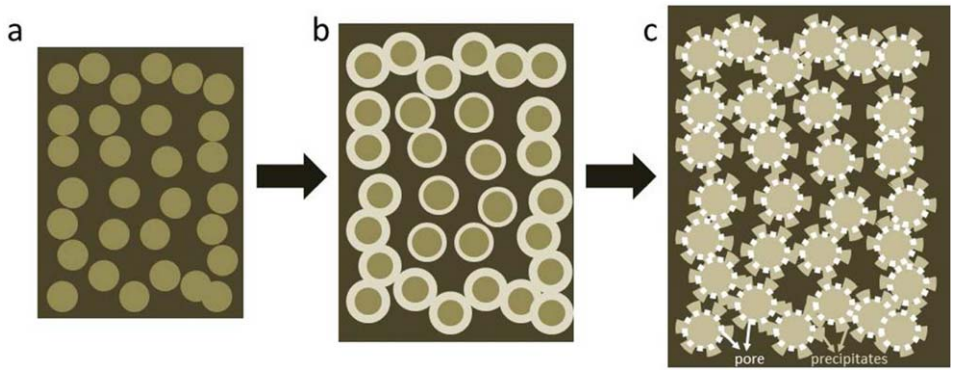

Figure 10. Schematic of MgO hydration in HNBR–MgO composites. (a) Before hydration, MgO particles are evenly distributed in the rubber matrix; (b) At the early hydration stage, MgO particles are hydrated on the surface layer and are connected, with increased E of the composites; (c) Fully hydrated: with more pores (filled with or without unreacted water) formation and precipitation of $Mg(OH)_2$ the connection between particles breaks, E of the composites decreases. The size of the schematic samples gives an idea of the sample volume evolution. [Color figure can be viewed in the online issue, which is available at wileyonlinelibrary.com.]

still much higher than the initial modulus of the composites (22 MPa, measured via nanoindentation). Therefore, MgO particles in the center of the composites already began to hydrate after immersing in water for 24 h. At this stage, the local modulus is proportional to the degree of hydration, that is, the higher degree of hydration, the larger modulus is.

After 51 h of swelling, the local elastic modulus increases in the center of the composites, with a slight decrease of E near the edges [Figure 9(b,e)]. For example, the average E at $x = 0 - 50$ μm decreased from 320 ± 27 MPa to 234 ± 19 MPa (decrease of 27%). At this time, the macroscale elastic modulus of the composites also decreased roughly 26% compared to its peak value at $t = 24$ h [Figure 1(b)]. The modulus map [Figure 9(c,f)] acquired at 96 h is also consistent with the macroscale modulus trend shown in Figure 1(b). After 96 h of swelling, the elastic modulus of the composite becomes uniform throughout its thickness, with an overall lower average modulus in each row of 109 ± 10 MPa, comparing to the average moduli at $t = 51$ h of 216 ± 17 MPa. In the later stage, the modulus is no longer proportional to the degree of hydration.

The nanoindentation results confirmed that for the first 24 h, the hydration is a diffusion driven process. If water is present, hydration takes place, and the composite becomes stiffer locally. Between 24 and 51 h, hydration of MgO is completed, but the swelling of water still proceeds and the modulus decreases macroscopically. In fact, both the macroscopic DMA and microscopic nanoindentation tests demonstrate that once the hydration of MgO reaches certain value, the additional water exposure leads to a decrease in modulus. We hypothesize here that this modulus drop is related to the presence of unreacted water around and inside the hydrated fillers. Previous research showed that during the hydration of MgO, pores form associated with the precipitation of $Mg(OH)_2$.[13,14] After MgO is fully reacted, water can still diffuse into the composites through the pores, and the pores do not all collapse even after the unreacted water is removed.[3] Figure 10 is a tentative schematic to illustrate our hypothesis. At the early stage of hydration, MgO reacts with water and the volume of the filler increases, causing the volume expansion of composite. Little or no unreacted water is present: all available water is used to react with MgO to form $Mg(OH)_2$ and the porosity of the fillers is low. This is illustrated in Figure 10(a,b). At this stage, hydration directly follows water diffusion, and the inhomogeneities are presented. The modulus locally reached very high values, potentially due to hydrated fillers connecting with each other and forming a network structure. With further water diffusion, and faster diffusion (we have shown that diffusivity increases with the extent of hydration in Water Diffusion and MgO Hydration Kinetics in HNBR-MgO Composite section), free water (i.e., unreacted water) starts accumulating in the sample. Because of the hydrophobic nature of HNBR, it is likely the water will accumulate around or inside the pores of the fillers, as shown in Figure 10(c). Having free water between the fillers and the rubber as well as inside the fillers may potentially break them to form precipitates, as shown in Figure 3(b,c)[13,14] or disrupt the filler network. This results in the decrease of local modulus, and finally overall modulus. Further experimental proof of the breakage of the connected filler structure is needed and it is beyond the scoop of the current work.

CONCLUSIONS

In this study, we investigated the hydration kinetics and the stiffening mechanism for HNBR-MgO reactive composites at microscale. The imhomegeneous MgO hydration within the composites was observed using SEM imaging. This inhomogeneous hydration in composites was measured and the water diffusion coefficient as a function hydration was determined with a numerical model. We found that the hydration of fillers can increase water-diffusivity orders of magnitude. We also demonstrated the uneven modulus evolution of the composites during initial swelling using instrumented grid indentation and shown that after the hydration reaches certain value, the additional water exposure leads to a decrease in modulus. This work provides the first study on the swelling/hydration kinetics of this novel reactive composite, which stiffens during swelling, at the microscopic level. This work can be expanded to examine the HNBR-MgO reactive composites with more complicated geometries and under different swelling conditions.

ACKNOWLEDGMENTS

The authors would like to acknowledge Schlumberger for its support and permission to publish. We thank our colleagues Xiaohong Ren, Henghua Jin, Travis Hohenberger for their valuable comments. We also acknowledge Alan Schwartzman and Konrad J Krakowiak from MIT for their help with nanoindentation experiments.

REFERENCES

1. Calvert, P. *Adv. Mater.* **2009**, *21*, 743.
2. Xie, Li, Z.; Chen, M.; Tu, X.; Li, H. S. *J. Appl. Polym. Sci.* **1996**, *61*, 495.
3. Han, Qu, D. M.; Yue, C.; Lou, Y.; Musso, Y.; Robisson, S. A. *Compos. Sci. Technol.* **2014**, *99*, 52.
4. Mostata, Abouel-Kasem, A. A.; Bayoumi, M. R.; El-Sebaie, M. G. *Mater. Des.* **2009**, *30*, 1561.
5. Robisson, A.; Maheshwari, S.; Musso, S.; Thomas, J. J.; Auzerais, F. M.; Han, D.; Qu, M.; Ulm, F. J. *Compos. Sci. Technol.* **2013**, *75*, 77.
6. Zhou, M. H.; ha, C. S.; Cho, W. *J. Appl. Polym.* **2001**, *81*, 1277.
7. Jakes, J. E.; Frihart, C. R.; Beecher, J. F.; Moon, R. J.; Resto, P. J.; Melgarejo, Z. H.; Suarez, O.; Baumgart, M. H.; Elmustafa, A. A.; Stone, D. S. *J. Mater. Res.* **2009**, *24*, 1016.
8. Soifer, Y.; Verdyan, M.; Kazakevich, A.; Rabkin, M. E. *Mater. Lett.* **2005**, *59*, 1434.
9. Fischer-Cripps, A. C. Nanoindentation, 3rd ed., Springer, **2011**.
10. Pharr, G. M.; Oliver, W. C.; Brotzen, F. R. *J. Mater. Res* **1992**, *7*, 613.
11. Fick, A. *Phil. Mag.* **1855**, *10*, 31.
12. Seignol, J. F.; Baghdadi, N.; Toutlemonde, F. The first international conference on computational Technologies in Concrete Structures (CTCS'09), France, **2009**.
13. Fruhwirth, O.; Herzog, G.; Hollerer, W.; Rachetti, I. A. *Surf. Technol.* **1985**, *24*, 301.
14. Khangaonkar, P.; Othman, R.; Ranjitham, R. M. *Minerals Eng.* **1990**, *3*, 227.